Journal of Medicinal Chemistry

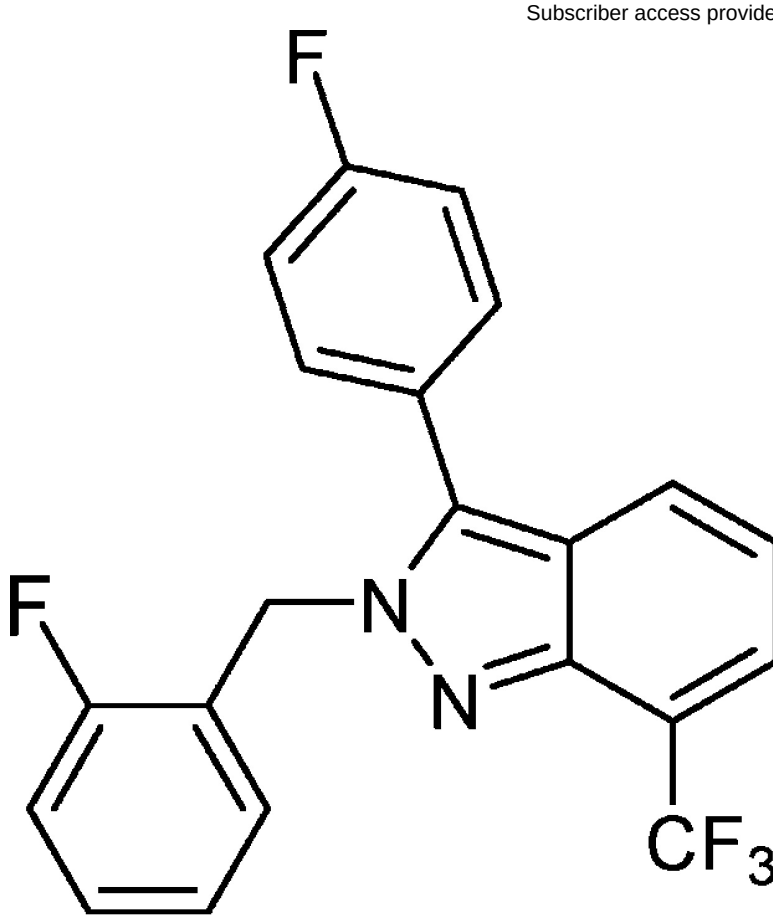

13

More About This Article

Additional resources and features associated with this article are available within the HTML version:

- Supporting Information
- Access to high resolution figures
- Links to articles and content related to this article
- Copyright permission to reproduce figures and/or text from this article

View the Full Text HTML

Journal of Medicinal Chemistry is published by the American Chemical Society.
1155 Sixteenth Street N.W., Washington, DC 20036

Indazole-Based Liver X Receptor (LXR) Modulators with Maintained Atherosclerotic Lesion Reduction Activity but Diminished Stimulation of Hepatic Triglyceride Synthesis[||]

Jay Wrobel,*[,†] Robert Steffan,[†] S. Marc Bowen,[†] Ronald Magolda,[†] Edward Matelan,[†] Rayomand Unwalla,[†] Michael Basso,[‡] Valerie Clerin,[‡] Stephen J. Gardell,[‡] Ponnal Nambi,[‡] Elaine Quinet,[‡] Jason I. Reminick,[▽] George P. Vlasuk,[‡] Shuguang Wang,[‡] Irene Feingold,[§] Christine Huselton,[§] Tomas Bonn,[#] Mathias Farnegardh,[#] Tomas Hansson,[#] Annika Goos Nilsson,[#] Anna Wilhelmsson,[#] Edouard Zamaratski,[#] and Mark J. Evans[‡]

Wyeth Pharmaceuticals, 500 Arcola Road, Collegeville, Pennsylvania 19426, and Karo Bio AB, Huddinge, Sweden

Received July 2, 2008

A series of substituted 2-benzyl-3-aryl-7-trifluoromethylindazoles were prepared as LXR modulators. These compounds were partial agonists in transactivation assays when compared to **1** (T0901317) and were slightly weaker with respect to potency and efficacy on LXRα than on LXRβ. Lead compounds in this series **12** (WAY-252623) and **13** (WAY-214950) showed less lipid accumulation in HepG2 cells than potent full agonists **1** and **3** (WAY-254011) but were comparable in efficacy to **1** and **3** with respect to cholesterol efflux in THP-1 foam cells, albeit weaker in potency. Compound **13** reduced aortic lesion area in LDLR knockout mice equivalently to **3** or positive control **2** (GW3965). In a 7-day hamster model, compound **13** showed a lesser propensity for plasma TG elevation than **3**, when the compounds were compared at doses in which they elevated ABCA1 and ABCG1 gene expression in duodenum and liver at equal levels. In contrast to results previously published for **2**, the lack of TG effect of **13** correlated with its inability to increase liver fatty acid synthase (FAS) gene expression, which was up-regulated 4-fold by **3**. These results suggest indazoles such as **13** may have an improved profile for potential use as a therapeutic agent.

Cardiovascular risk is increased in patients with dyslipidemia, diabetes, and the metabolic syndrome. In spite of the wide availability and use of effective lipid-lowering and glucose-lowering therapies, cardiovascular disease remains the leading cause of morbidity and mortality in the industrialized world. Liver X receptors (LXRs[a]) belong to a transcription factor subfamily that consists of LXRα (expressed in adipose, intestine, liver, kidney, and macrophages) and LXRβ (expressed ubiquitously).[1−4] Oxysterols are endogenous ligands for LXR. Ligand binding results in exchange of corepressors and coactivators associated with LXR−RXR heterodimers that are bound to DNA response elements. LXR-mediated gene expression has been shown to induce reverse cholesterol transport (RCT)−cholesterol efflux from macrophages via ApoE and ATP-binding cassettes (ABC transporters ABCA1, and ABCG1), and to enhance bile acid production in mice. In mice, the loss of LXR expression increases atherosclerosis,[5] while conversely, treatment of mice with an LXR agonist reduces atherosclerosis development.[6] An LXR agonist may offer potential benefits on lipid metabolism, improving glucose metabolism and vascular inflammation and thereby reducing the risk of cardiovascular disease. Specifically, LXR agonists may increase insulin sensitivity, suppress gluconeogenic genes, and antagonize the expression of inflammatory genes (e.g., iNOS, IL-1B, IL-6, and COX2), as well as enhance reverse cholesterol transport, all contributing to the possibility of reduced morbidity and mortality in patients with established atherosclerosis. Known LXR modulators such as **1** (TO901317)[7] and **2** (GW3965)[6,8] (Figure 1) up-regulate LXR target genes in vivo and retard the advancement of atherosclerotic processes in mouse models of atherosclerosis. However, these compounds also induce hypertriglyceridemia by LXRα induction of genes in the liver involved in fatty acid biosynthesis, including sterol regulatory binding element protein 1c (SREBP-1c) and fatty acid synthase (FAS).[7] The pharmacological challenge, therefore, is to identify LXR modulators that selectively activate desirable LXR target genes.

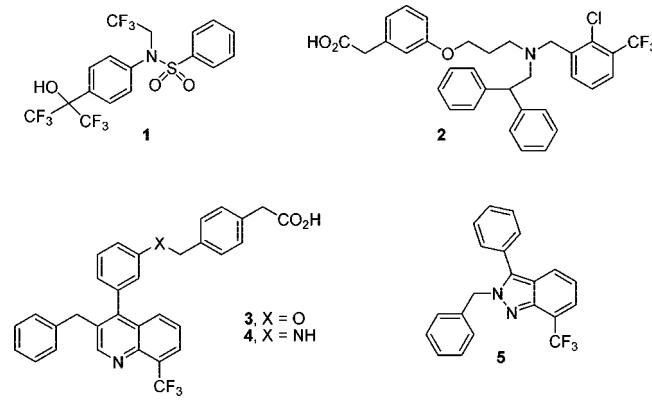

Figure 1. Known LXR agonists and the indazole lead.

Previous drug design efforts to improve the pharmaceutical properties of an early quinoline lead series led to the preparation potent phenylacetic acid substituted quinolines represented by **3** (WAY-254011)[9] and **4**.[9,10] Both compounds significantly

[||] Dedicated to the memory of Dr. Ronald Magolda.

* To whom the correspondence should be addressed. Phone: 484-865-2480. Fax: 484-865-9399. E-mail: wrobelj@wyeth.com.

[†] Chemical and Screening Sciences, Wyeth Pharmaceuticals.

[‡] Cardiovascular and Metabolic Diseases, Wyeth Pharmaceuticals.

[▽] Translational Medicine, Wyeth Pharmaceuticals.

[§] Drug Metabolism, Wyeth Pharmaceuticals.

[#] Karo Bio AB.

[a] Abbreviations: LXR, liver X receptor; ABCA1/G1, adenosine triphosphate binding cassette, A1/G1; HepG2, human hepatocellular liver carcinoma cell line; THP-1, human acute monocytic leukemia cell line; LDLR, low density lipoprotein receptor; TG, triglycerides; RXR, retinoic acid X receptor; RCT, reverse cholesterol transport; SREBP-1c, sterol regulatory binding element 1c; FAS, fatty acid synthase; LBD, ligand binding domain; PPARs (α, γ, or δ), peroxisome proliferator-activated receptor α, γ, or δ; FXR, farnesoid X receptor; PXR, pregnane X receptor; TR, thyroid receptor; cyp7A1, cytochrome P450 7A1 hydroxylase; CETP, cholesterol ester transfer protein; DMF, dimethylforamide, EtOAc, ethyl acetate.

10.1021/jm800799q CCC: $40.75
Published on Web 10/31/2008

Table 1. LXR Activity of Indazoles of General Structure **10**[a]

compd	Y	R_1	R_2	LXRβ binding[b]	LXRα binding[b]	Gal4 LXRβ[c]	Gal4 LXRα[c]
1				9	13	0.17 (100)	0.14 (100)
				$n = 5$	$n = 3$	$n = 177$	$n = 177$
2				12	100	0.31 (77)	0.66 (58)
				$n = 7$	$n = 7$	$n = 5$	$n = 5$
3				2	10	0.09 (63)	0.24 (90)
				$n = 15$	$n = 15$	$n = 3$	$n = 3$
4				2	8	0.09 (70)	0.16 (82)
				$n = 3$	$n = 3$	$n = 3$	$n = 3$
5	H	H	H	41	279	3.26 (53)	4.27 (31)
				$n = 5$	$n = 5$		$n = 1$
11	F	Me	Me	10	78	0.99 (75)	1.81 (58)
							$n = 1$
12	F	Cl	F	24	179	3.67 (73)	6.66 (53)
				$n = 8$	$n = 8$	$n = 12$	$n = 12$
13	F	F	H	33	248	4.15 (64)	6.10 (35)
				$n = 9$	$n = 9$	$n = 13$	$n = 13$
14	F	Cl	H	32	297	2.89 (54)	5.02 (32)
				$n = 8$	$n = 8$	$n = 3$	$n = 3$
15	F	H	F	49	317	5.72 (66)	8.40 (43)
16	F	H	Cl	58	401	9.05 (74)	12.77 (35)
17	Cl	F	Cl	38	260	9.80 (104)	13.28 (64)
18	Cl	Cl	F	30	252	11.22 (77)	14.40 (45)
19	Cl	Cl	H	40	379	10.2 (67)	15.21 (36)
20	Cl	F	H	38	304	7.44 (68)	13.44 (50)
21	Cl	CF_3	H	48	465	15.46 (38)	15.83 (5)
22	Cl	H	CF_3	1853	3101	NT	NT
				$n = 1$	$n = 1$		

[a] Results are given as the mean of two independent experiments unless otherwise indicated. [b] IC_{50} in nM. The standard deviations for these assays were typically ±30% of the mean or less. [c] EC_{50} in μM (% efficacy). The standard deviations for these assays were typically ±50% of the mean or less. The % of efficacy is relative to that of **1**. NT = not tested.

reduced lesion size in an atherosclerosis mouse model (8-week LDLR −/− mouse model) at 10 mg/kg.[8,11,12] However, **3** also caused substantial liver and plasma triglyceride (TG) increases in hamster (vide infra). These compounds were potent full agonists for both LXR isoforms (relative to a standard LXR modulator **1**). The growing body of evidence supports the hypothesis that the lipogenic effects in liver are primarily LXRα mediated.[13,14] Furthermore, both isoforms play a role in macrophage RCT processes and atherosclerosis but the LXRβ isoform alone may be sufficient for these processes.[13,15,16] Thus, a more desired profile for a compound would be one that minimizes the agonist activity due to the LXRα isoform and maximizes the LXRβ agonist activity.[16] With this premise our medicinal chemistry efforts focused on finding compounds with reduced LXRα agonist activity.

In this regard, our indazole-based series (lead candidate **5**) showed promise as a series to explore for optimization. Compound **5** had an IC_{50} value of 41 nM for binding to LXRβ and was a partial agonist on LXRα according to our transactivation assay (Table 1). This compound is structurally analogous to quinoline series members such as **3**[9] and can be viewed as collapse of the 6/6 quinoline ring system to a 6/5 indazole system. However, compound **5** was rapidly metabolized in mouse, rat, and human microsomes and subsequent PK studies in mouse revealed that the compound had high clearance, low drug levels, and poor oral bioavailability. Metabolic identification studies indicated that the primary metabolite was oxidative metabolism on the phenyl rings. Thus, the optimization of ADME and PK parameters of compound **5** became a primary area of focus. Herein, we describe analogues of **5** with improved metabolic stability and their subsequent LXR activity in vitro and in a hamster lipid and mouse atherosclerosis model.[17,18]

Chemistry

The synthesis of the indazole analogues related to **5** is shown in Scheme 1. The commercially available 2-fluoro-3-trifluoromethylbenzoic acid was converted to the Weinreb amide under standard means and reacted with *p*-fluoro- or *p*-chlorophenylmagnesium bromide to afford the 2-fluorobenzophenones **7**. Reaction of **7** with hydrazine led to indazoles **8**. Heating **8** with the appropriate benzyl bromide **9** in DMF with the exclusion of a base led to the N2 alkylated indazoles **10** with no or very little N1 alkylation. The NMR spectra for the N2 analogues displayed a typical pattern distinct from the N1 substituted regioisomers. In the case of compound **14** the proton at position 4 displays a doublet at δ 7.85, whereas in the regioisomer substituted at N-1 the same proton displays a doublet at δ 8.39. A ^{1}H NMR NOESY spectrum for compound **14** was obtained confirming N2 substitution (see Supporting Information). Further evidence of N2 substitution is confirmed in the X-ray crystal structure of compound **12** (Figure 3).

Scheme 1[a]

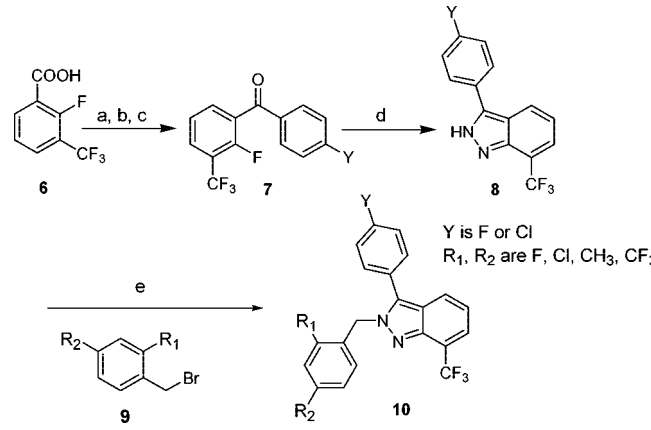

[a] Reaction conditions: (a) $(COCl)_2$, 95%; (b) NH(OMe)Me·HCl, K_2CO_3, toluene, water, 100%; (c) *p*-fluoro- or *p*-chlorophenylmagnesium bromide, THF, 0 °C to room temp; (d) $NH_2NH_2 \cdot H_2O$, THF, 55−65 °C, 8 h, 77%; (e) compound **9**, DMF, 120 °C, 60−90%.

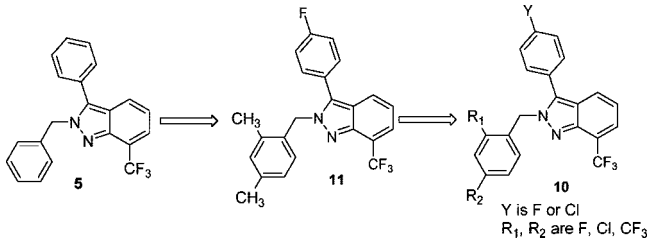

Figure 2. Path toward metabolically stable analogues of **5**.

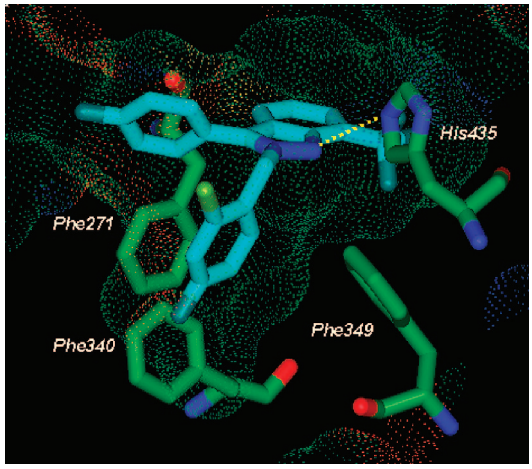

Figure 3. X-ray crystal structure of **12** bound to LXRβ. Only key residues involved in ligand interaction are shown for clarity. Hydrogen bonds to key residues are shown as yellow dotted lines.

Results and Discussion

The LXR binding activities of compounds were evaluated (Table 1) using recombinant human LXRα or LXRβ ligand binding domains (LBDs) with [^{3}H]**1** as a tracer. Huh-7 human hepatoma cell based Gal4 LXRα or LXRβ transactivation assays were used to assess the agonist potency and efficacy. Efficacy in this assay is relative to **1**, which is defined as 100%. SAR studies on the indazole series revealed that small lipophilic substituents on the 2-benzyl moiety enhanced potency. For example, compound **11** (Figure 2) with 2′, 4′-dimethyl groups on the 2-benzyl moiety had a LXRβ binding IC_{50} of 10 nM. Like **5**, this compound showed rapid in vitro metabolism and poor PK parameters in mice [high clearance (Clp), low exposure (AUC), and low oral bioavailability (% *F*)]. However, oxidative metabolism was now shunted toward the methyl groups of the 2-(2′, 4′-dimethyl)benzyl substituent although the *p*-fluorine substituent of **11** impeded oxidative metabolism at the 3-phenyl ring. Replacement of the dimethyl groups of **11** with halogens led to compounds (**12**−**22**) with increased metabolic stability and improved PK parameters.

Compounds **12**−**16**, like compound **11**, contain a *p*-fluoro substituent on the indazole 3-phenyl ring (i.e. Y = F). However, the benzyl moiety of **12**−**16** contained chloro, fluoro, or hydrogen in place of the dimethyl groups of **11**. These compounds were slightly weaker binders on both LXRβ (IC_{50} values of of 24−58 nM) and LXRα (IC_{50} values of 179−401 nM) compared to **11**, and this translated to weaker transactivation potencies, although the efficacy on LXRβ or LXRα was similar to that for **11**. The position or type (Cl or F) of the halogen (R_1 or R_2) did not have much effect on the binding or transactivation potencies of the compound with the exception of a p-chloro group (R_2 = Cl), which resulted in a slightly weaker potency compound (**16**). Congeners with a 3-(*p*-chloro)phenyl group (**17**−**20**) had similar binding potencies compared to the 3-(*p*-fluoro)phenyl containing compounds (**12**−**16**); however, they were less potent agonists. The analogues with trifluoromethyl groups (**21** and **22**) showed reduced potency relative to compounds with chloro or fluoro groups. Compound **22** was an exceptionally weak binder, most likely because of steric and electronic effects within the LBD.

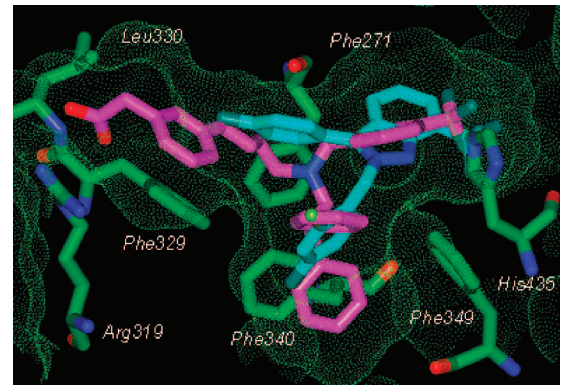

Figure 4. X-ray crystal structure of hLXRβ complexed with **12** (colored cyan) overlaid with published X-ray structure of compound **2** (colored magenta). Only key residues within the binding site are shown from **2**.

Table 2. Cellular Activity of Selected Compounds[a]

compd	ABCA1[b]	C-efflux[c]	SREBP1c[d]	lipid accum[e]
1	44 (100) $n = 203$	3 (100) $n = 3$	61 (100) $n = 14$	137 (100) $n = 73$
2	434 (178) $n = 4$	31 (84)	210 (137)	2002 (45) $n = 3$
3	84 (155) $n = 8$	6 (88) $n = 4$	120 (96)	223 (85) $n = 3$
12	541 (100) $n = 3$	1275 (140) $n = 5$	2114 (58)	1911 (35) $n = 3$
13	551 (89) $n = 4$	549 (132)	1222 (72)	998 (38)

[a] EC_{50} in nM (% efficacy). Results are given as the mean of two independent experiments unless otherwise indicated. The standard deviations for these assays were typically ±50% of the mean or less. The % of efficacy is relative to that of **1**. [b] In differentiated THP-1 cells. [c] In differentiated THP-1 cells loaded with ac-LDL and labeled with [^{3}H]cholesterol representing atherosclerotic foam cells. [d] In HepG2 cells. [e] Lipid accumulation is measured in HepG2 cells.

An X-ray structure of **12** bound to the LXRβ ligand-binding domain was also obtained (Figure 3).[19] There are many similarities to previously published structure of **3**.[9] Ligand recognition was achieved by multiple interactions that line the pocket, the N1 indazole nitrogen formed a H-bond interaction with the Nϵ(epsilon) of His435, while the 7-trifluoromethyl group, being in proximity, made attractive electrostatic interactions; i.e., d(N−F) = 2.9 Å with this residue. The N2-benzyl group was enclosed in a hydrophobic pocket surrounded by three Phe residues (271, 340, and 349). This structure provides a plausible explanation for the weak potency of compound **22**. In compound **22** the *p*-fluoro moiety of the 2-benzyl group of **12** is replaced by the more bulky and electronegative trifluoromethyl moiety. This would place the CF_3 group of **22** near the π-cloud of Phe340 residue and lead to an unfavorable electrostatic stacking interaction.

Interestingly, an overlay of X-ray structure of **12** with published structure of a larger LXR ligand, i.e., **2**[20] (Figure 4)[19] revealed important differences in their interactions with the receptor. Although both ligands induced an agonist conformation of helix H12, the binding pocket of **2** was considerably larger and different from that of **12**. The carboxylic acid group of **2**

Table 3. PK Parameters for Compounds **5** and **13** in C57 Male Mice[a]

compd	iv $t_{1/2}$ (h)	Cl ((mL/min)/kg)	V_{ss} (L/kg)	po $t_{1/2}$ (h)	C_{max} (ng/mL)	T_{max} (h)	$AUC_{(0-\infty)}$ (h·ng/mL)	F (%)
5	1.9	81	5.2	2.2	124	0.25	321	16
13	7.9	57	30.3	5.8	633	0.5	3101	106

[a] Single dose PK study done in male C57 mice (weight 20−35 g). For iv, compound was given at 1 mg/kg in 2% ethanol, 40% PEG200 in saline. For po, compound was given at 10 mg/kg in 0.5% methylcellulose, 2% Tween-80 in water. Dose volume for iv and po studies was 5 mL/kg.

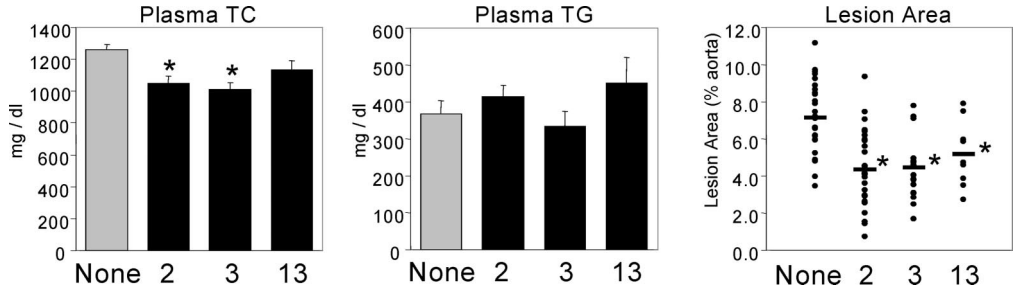

Figure 5. Male LDLR −/− mice were fed a Western diet (gray bars, $n = 28$) or diet supplemented to deliver 10 mg/kg compound **2** ($n = 28$), 10 mg/kg compound **3** ($n = 20$), or 15 mg/kg compound **13** ($n = 9$). After 8 weeks, plasma total cholesterol (TC) and total triglyceride (TG) were determined using a Roche 911 clinical chemistry analyzer. Values are the mean ± SEM. Aortic lesion area was determined by en face analysis of Oil Red O stained aortas. Lesion size in each individual animal is shown (filled circles) along with the group mean (lines): (∗) $p < 0.05$ vs control animals by ANOVA.

was able to extend out to the β-hairpin loop and make additional interactions with residues from this region, i.e., Arg319 and the NH backbone of Leu330 residue. By reaching into this cavity, compound **2** was further able to stabilize this flexible region over compound **12**. Additionally, the diphenylethyl chain of **2** induced small shifts within the side chain residues lining the hydrophobic pocket, i.e., phe271, phe340, and phe349 in order to accommodate this larger group. Taken together, these observed differences in the binding pocket might explain why compound **2** has increased binding and transactivation potency over compound **12**.

Compounds **12** (WAY-252623) and **13** (WAY-214950) were among the most potent and stable of the compounds **12**−**22** showing reduced LXRα agonism, and so these two compounds were further profiled in gene regulation and functional assays to better assess their ability to promote the desired reverse cholesterol transport activity (ABCA1 expression in THP-1 cells and cholesterol efflux in macrophage-like foam cells) in relation to undesired TG synthesis activities (SREBP1c expression and lipid accumulation in HepG2 liver cells). The data are shown in Table 2. Literature compounds **1** and **3**, which are potent full agonists for LXRα and LXRβ in the transactivation assays, showed little differentiation between cellular reverse cholesterol transport in macrophage cells versus cellular TG synthesis in HepG2 cells. In contrast, treatment of cells with either **12** or **13** increased ABCA1 gene expression in THP-1 cells with similar full efficacy, albeit with lower potency than **1** or **3**. However, **12** or **13** were partial agonists and had weaker potency for increasing SREBP1c mRNA in liver cells compared to **1** or **3**. An LXR modulator having this profile may have less liability with respect to TG synthesis versus promoting reverse cholesterol transport.

The gene expression data were borne out in cellular functional assays. Compounds **12** and **13** stimulated [^{3}H] cholesterol efflux in THP-1 foam cells in a concentration-dependent manner. The compounds were as efficacious as **1** or **3** although not as potent in this assay. On the other hand, **12** or **13** showed relatively poor efficacy (and potency) relative to the full agonists **1** and **3** with respect to TG accumulation in HepG2 cells and had reduced potency for SREBP-1c induction. The differential activities on liver cells and macrophages are a favorable profile for an LXR modulator.

Compounds **12** and **13** did not display agonist activity against PPARs (α, γ, or δ) and FXR and were >40-fold (for **12**) and >65 fold (for **13**) less potent, based on binding IC_{50} values over PXR, RXR, GR, MR, AR, PR, ER, and TR over LXRβ (see Supporting Information for details).

Compound **13** showed acceptable PK parameters in C57 mice (Table 3). Following an iv dose, the half-life was long, the clearance was moderate, and the volume of distribution was high. Following an oral dose, the terminal half-life was long and the oral bioavailablity was high. This was in contrast to the des-halogen early indazole lead **5**, which had high clearance, low oral bioavailability, and much lower exposure and C_{max} relative to **13**, thus proving that halogenation protects the molecule from rapid metabolism.

Synthetic LXR agonists such as compound **2** significantly reduce atherosclerotic lesion size in LDLR −/− mice. To compare the in vivo activity of selected compounds, male LDLR −/− mice were fed a Western diet or Western diet supplemented with **2**, **3**, or **13** for a period of 8 weeks.[21] Compound **2** reduced total cholesterol levels by 17%, had no effect on plasma triglyceride level, and reduced lesion size by 40% (Figure 5), nearly identical to published results of 18% total cholesterol reduction, no TG effect, and 34% lesion reduction.[6] Compound **3** produced very similar results, lowering plasma total cholesterol by 20%, having no effect on plasma triglyceride levels, and reducing lesion size by 38%. Compound **13** produced a nonsignificant 10% decrease in total cholesterol, had no effect on plasma triglyceride levels, and reduced lesion size by 28%. Compound treatment did not affect animal weights. There was no significant difference between the magnitude of lesion reduction by **2**, **3**, or **13**. Thus, all three LXR agonists similarly reduced lesion size without producing any detrimental plasma lipid effects.

In addition, the effects of compound **13** on LXR responsive genes were monitored in several tissues. In the duodenum ABCA1 gene expression was up-regulated (2.3 ± 0.14)-fold by **13** and (6.9 ± 0.08)-fold by compound **2**. In the liver, CYP7A1, which is regulated by LXR only in mice, was increased (4.0 ± 0.10)-fold by compound **13** and (1.9 ± 0.14)-fold by **2**.

Although LXR agonists such as **2** favorably reduced atherosclerotic lesion size in mice, in species such as the hamster and

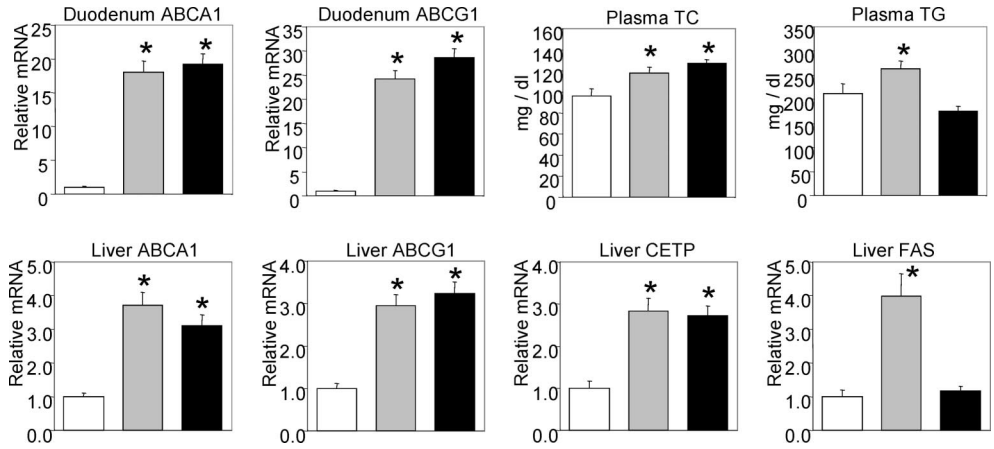

Figure 6. Male Golden Syrian hamsters were treated by oral gavage with 1 mL of 0.5% methylcellulose/2% polysorbate (Tween) 80 vehicle (open bars), 3 mg/kg compound **3** in vehicle (gray bars), or 100 mg/kg compound **13** in vehicle (black bars) for 7 days. On the final day, food was removed at time of final dosing. Two hours later the animals were euthanized. RNA was prepared from duodenum and liver and quantified by real time PCR. All gene expression values were normalized for glyceraldehyde-3-phosphate dehydrogenase (GAPDH) expression, with the expression seen in vehicle treated animals defined as 1.0 for each gene. Plasma total cholesterol and triglyceride were determined using a Roche 912 clinical chemistry analyzer: (∗) $p < 0.05$ vs vehicle control.

primates, compound **2** elevated plasma triglyceride as well as plasma total and LDL cholesterol but lowered HDL cholesterol.[22] The basis for this effect may be due to LXR induction of cholesterol ester transfer protein (CETP) expression in these species. To determine whether compounds **3** and **13** produced similar lipid effects, hamsters fed a standard chow diet were treated with 3 mg/kg compound **3** or 100 mg/kg compound **13.** These doses were chosen to produce equivalent induction of ABCA1 and ABCG1 expression in both the duodenum and the liver (Figure 6). Both compounds **3** and **13** produced equivalent increases in plasma total cholesterol levels, and both compounds produced identical increases in hepatic CETP expression. In contrast, while compound **3** increased plasma triglyceride levels by 25%, compound **13** had no effect on plasma triglyceride levels.[23] Neither compound showed a hepatic TG increase at these doses. Hepatic expression of fatty acid synthase (FAS), the rate limiting enzyme for triglyceride synthesis in the liver, was induced 4-fold by compound **3** but was not induced by compound **13**. Together, these results suggest that LXRα partial agonist compound **13** has a reduced propensity to elevate plasma triglycerides compared to other synthetic LXR agonists in the hamster, potentially due to a selective gene regulation profile in the liver.

Conclusion

Indazoles **5**−**21** were partial agonists in transactivation assays, particularly on LXRα relative to full agonists **1**−**4**. Despite their partial agonism in transactivation assays, compounds **12** and **13** showed full agonism (relative to **1**) in THP-1 cells with respect to increasing ABCA1 gene expression and on cholesterol efflux in THP-1 foam cells compared to **1**−**3**. These in vitro LXR activities of **13**, although lower in potency than **1** or **3**, were sufficient to translate to in vivo activities, since the compound showed reduction of aortic arch lesion progression and stimulation of LXR genes in the duodenum and liver in LDLR −/− mice. Compounds **12** and **13** also showed less potential for triglyceride elevation over full agonists such as **1** and **3**. The compounds were partial agonists in HepG2 cells with respect to up-regulation of SREBP1-c, a gene involved in liver TG synthesis, and were less efficient in promoting lipid accumulation in this cell type. This translated to an inability of **13** to increase plasma triglyceride levels or liver FAS gene transcription in hamster relative to the potent LXR agonist **3** when both compounds were administered at doses that generate comparable ABC transporter gene activity. Thus, our premise of minimizing LXRα agonist efficacy while maintaining LXRβ efficacy was shown to provide compounds that retain antiatherosclerosis benefits of LXR agonists while reducing the unwanted lipid effects of these agonists.

Experimental Section

General. Solvents and chemicals were purchased from EM Sciences, VWR, Oakwood, and Aldrich Chemical Co. and used without further purification. MS results were obtained on an Agilent MS. High-resolution mass spectra were obtained on a Waters LC−TOFMS instrument and were measured to within 5 ppm of calculated values. ^{1}H NMR spectra were obtained on a Varian (400 MHz) instrument. NMR data are given as δ values (ppm) using tetramethylsilane as an internal standard ($\delta = 0$ ppm).

2-(2,4-Dimethylbenzyl)-3-(4-fluorophenyl)-7-(trifluoromethyl)-2*H*-indazole (11). Step 1: Preparation of (2-Fluoro-3-(trifluoromethyl)phenyl)(4-fluorophenyl)methanone. A solution of 2-fluoro-3-trifluoromethylbenzoic acid (10 g, 65 mmol) and oxalyl chloride (5.7 mL, 65 mmol) in 100 mL of dry CH_2Cl_2 was treated with a few drops of DMF. The solution was stirred at ambient temperature for 1 h. In one portion was added *N*,*O*-dimethylhydroxylamine hydrochloride (16.8 g, 174 mmol) followed by 16 mL of pyridine dropwise. The mixture was stirred for 48 h at ambient temperature. The mixture was partitioned with H_2O. The organic phase was washed with 2 N HCl, brine and was dried with Na_2SO_4. Concentration of the organic phase resulted in 13.3 g of the intermediate 2-fluoro-*N*-methoxy-*N*-methyl-3-(trifluoromethyl)-benzamide as a clear oil.

To a stirred solution of 2-fluoro-*N*-methoxy-*N*-methyl-3-(trifluoromethyl)benzamide (12.8 g, 65 mmol) in 150 mL of THF was added 4-fluorophenylmagnesium bromide (2 N in diethyl ether, 32.5 mL, 65 mmol), and the mixture was heated at 50 °C overnight. The reaction mixture was partitioned with EtOAc and H_2O. The organic phase was dried (Na_2SO_4) and concentrated in vacuo. The residue was purified by flash chromatography (silica gel, hexane/CH_2Cl_2, 3:1) to give the title compound (9.78 g, 52% yield). ^{1}H NMR (DMSO-d_6, 400 MHz) δ 7.43 (t, 2 H, $J = 8.83$ Hz), 7.61 (t, 1 H, $J = 7.81$ Hz), 7.82 (m, 3 H), 8.06 (t, 1 H, $J = 7.04$).

Step 2: Preparation of 3-(4-Fluorophenyl)-7-(trifluoromethyl)-1*H*-indazole. A solution of (2-fluoro-3-(trifluoromethyl)phenyl)(4-fluorophenyl)methanone (6.58 g, 23 mmol), hydrazine hydrate (7.36 mL, 230 mmol), and dimethylaminopyridine (2.8 g,

23 mmol) in 20 mL of pyridine was heated at 110 °C overnight. The reaction mixture was partitioned with EtOAc and H_2O. The organic phase was dried (Na_2SO_4) and concentrated in vacuo to give 8.0 g of crude yellow solid. The crude product was dissolve in CH_2Cl_2 and passed through a plug of silica gel. The plug was washed with additional CH_2Cl_2. The combined filtrate was concentrated in vacuo to give 5.18 g of product as a white solid (yield = 80%). ^{1}H NMR (DMSO-d_6, 400 MHz) δ 7.39 (t, 3 H, J = 8.84 Hz), 7.82 (d, 1 H, J = 7.3 Hz), 8.04 (m, 2 H), 8.37 (d, 1 H, J = 8.2 Hz), 13.81 (s, 1H); LC/MS 281.22 $[M + H]^+$.

Step 3: Preparation of 2-(2,4-Dimethylbenzyl)-3-(4-fluorophenyl)-7-(trifluoromethyl)-2*H*-indazole. A solution of 3-(4-fluorophenyl)-7-(trifluoromethyl)-1*H*-indazole (0.28 g, 1 mmol) and 2,4-dimethylbenzylmethane sulfonate (0.321 g, 1.5 mmol) in DMF was heated at 120 °C overnight. The reaction mixture was partitioned with EtOAc and H_2O. The organic phase was washed with brine and concentrated in vacuo. The crude residue was purified by flash chromatography (CH_2Cl_2) to give 0.117 g product as a white solid (yield = 29%). ^{1}H NMR (DMSO-d_6, 400 MHz) δ 2.17 (s, 3H), 2.19 (s, 3H), 5.67 (s, 2 H), 6.33 (s, 1H, J = 7.93 Hz), 6.83 (d, 1 H, J = 7.79 Hz), 6.97 (s, 1H), 7.23 (t, 1H, J = 7.8 Hz), 7.42 (m, 2H), 7.60 (m, 2H), 7.74 (d, 1H, J = 7.01 Hz), 7.83 (d, 1H, J = 8.45); MS (ESI) m/z 399 $[M + H]^+$. HRMS: calcd for $C_{23}H_{18}F_4N_2 + H^+$, 399.1479; found (ESI, $[M + H]^+$ obsd), 399.1481. Anal. ($C_{23}H_{18}F_4N_2$) C, H, N. HPLC purity: 100%.

2-(2-Chloro-4-fluorobenzyl)-3-(4-fluorophenyl)-7-(trifluoromethyl)-2*H*-indazole (12). A solution of 3-(4-fluorophenyl)-7-(trifluoromethyl)-1*H*-indazole (0.15 g, 0.54 mmol) and 2-chloro-4-fluorobenzyl bromide (0.134 g, 0.6 mmol) in DMF was heated at 120 °C overnight. The reaction mixture was partitioned with EtOAc and H_2O. The organic phase was washed with brine and concentrated in vacuo. The crude residue was purified by preparative HPLC over silica gel (Biotage 12M; hexane/methyl *tert*-butyl ether gradient, 5% methyl *tert*-butyl ether to 95% over 15 min at 10 mL/min) to give 0.106 g of product as a white solid (yield = 46%, mp 93 °C). ^{1}H NMR (DMSO-d_6, 400 MHz) δ 5.77 (s, 2H), 6.92 (m, 1H), 7.14 (dt, 1H), 7.24 (t, 1H, J = 7.8 Hz), 7.43 (m, 3H), 7.65 (m, 2H), 7.76 (d, 1H, J = 7.01 Hz), 7.83 (d, 1H, J = 8.45 Hz); MS (ESI) m/z 423 $[M + H]^+$. HRMS: calcd for $C_{21}H_{12}ClF_5N_2 + H^+$, 423.06819; found (ESI-FTMS, $[M + H]^{1+}$ 423.0683. Anal. ($C_{21}H_{12}ClF_5N_2$) C, H, N. HPLC purity 100%.

2-(2-Fluorobenzyl)-3-(4-fluorophenyl)-7-(trifluoromethyl)-2*H*-indazole (13). Reaction was run according to the procedure of compound **12** from 3-(4-fluorophenyl)-7-(trifluoromethyl)-1*H*-indazole (0.15 g, 0.54 mmol) and 2- fluorobenzyl bromide (0.113 g, 0.6 mmol) to give 0.103 g of product (yield = 49%, mp 89−90 °C). ^{1}H NMR (DMSO-d_6, 400 MHz) δ 5.77 (s, 2H), 6.93 (dt, 1H), 7.08−7.17 (m, 2H), 7.23 (t, 1H, J = 7.67 Hz), 7.31 (m, 1H), 7.43 (m, 2H), 7.63 (m, 2H), (dd, 1H), 7.83 (d, 1H, J = 8.44 Hz); MS (ESI) m/z 389 $[M + H]^+$. HRMS: calcd for $C_{21}H_{13}F_5N_2 + H^+$, 389.1072; found (ESI, $[M + H]^+$ obsd), 389.1081. Anal. ($C_{21}H_{13}F_5N_2$) C, H, N. HPLC purity: 100.0%.

2-(2-Chlorobenzyl)-3-(4-fluorophenyl)-7-(trifluoromethyl)-2*H*-indazole (14). Reaction run according to the procedure of compound **12** from 3-(4-fluorophenyl)-7-(trifluoromethyl)-1H-indazole (0.15 g, 0.54 mmol) and 2- chlorobenzylbromide (0.124 g, 0.6 mmol) to give 0.081 g product (yield = 37%). ^{1}H NMR (DMSO-d_6, 400 MHz) δ 5.80 (s, 2H), 6.765 (dd, 1H), 7.25 (dt, 1H), 7.31 (dt, 1H), 7.42 (m, 2H), 7.63 (m, 2H), 7.77 (dd, 1H), 7.84 (d, 1H, J = 8.44 Hz); MS (ESI) m/z 405 $[M + H]^+$; HRMS: calcd for $C_{21}H_{13}ClF_4N_2 + H^+$, 405.0776; found (ESI, $[M + H]^+$ obsd), 405.0782. Anal. ($C_{21}H_{13}ClF_4N_2$) C, H, N. HPLC purity: 100.0%.

2-(4-Fluorobenzyl)-3-(4-fluorophenyl)-7-(trifluoromethyl)-2*H*-indazole (15). Reaction was performed according to the procedure of compound **12** from 3-(4-fluorophenyl)-7-(trifluoromethyl)-1*H*-indazole (0.15 g, 0.54 mmol) and 4- fluorobenzyl bromide (0.113 g, 0.6 mmol) to give 0.085 g of product (yield = 40%). ^{1}H NMR (DMSO-d_6, 400 MHz) δ 5.72 (s, 2H), 7.03−7.14 (m, 4H), 7.23 (t, 1H, J = 7.67), 7.44 (m, 2H), 7.61 (m, 2H), 7.74 (d, 1H, J = 7.01 Hz), 7.81 (d, 1H, J = 8.44 Hz); MS (ESI) m/z 389 $[M + H]^+$. HRMS: calcd for $C_{21}H_{13}F_5N_2 + H^+$, 389.1076; found (ESI, $[M + H]^+$ obsd), 389.1072. Anal. ($C_{21}H_{13}F_5N_2$) C, H, N.

2-(4-Chlorobenzyl)-3-(4-fluorophenyl)-7-(trifluoromethyl)-2*H*-indazole (16). Reaction was performed according to the procedure of compound **12** from 3-(4-fluorophenyl)-7-(trifluoromethyl)-1*H*-indazole (0.15 g, 0.54 mmol) and 4-chlorobenzyl bromide (0.124 g, 0.6 mmol) to give 0.060 g of product (yield = 27%). ^{1}H NMR (DMSO-d_6, 400 MHz) δ 5.73 (s, 2H), 7.01 (d, 2H, J = 8.44 Hz), 7.23 (t, 1H, J = 7.80 Hz), 7.34 (d, 2H, J = 8.58 Hz), 7.43 (m, 2H), 7.61 (m, 2H), 7.75 (d, 1H, J = 7.01 Hz), 7.82 (d, 1H, J = 8.45 Hz); MS (ESI) m/z 405 $[M + H]^+$. HRMS: calcd for $C_{21}H_{13}F_4N_2 + Na^+$, 427.0592; found (ESI, $[M + Na]^+$ obsd), 427.0596. Anal. ($C_{21}H_{13}F_4N_2$) C, H, N. HPLC purity: 100%.

2-(4-Chloro-2-fluorobenzyl)-3-(4-chlorophenyl)-7-(trifluoromethyl)-2*H*-indazole (17). Step 1: Preparation of 3-(4-fluorophenyl)-7-(trifluoromethyl)-1*H*-indazole. A solution of (2-fluoro-3-(trifluoromethyl)phenyl)(4-chlorophenyl)methanone (10.5 g, 34.7 mmol, prepared as described above for 4-fluoroanalogue intermediate of **12**), hydrazine hydrate (11 mL, 347 mmol), and dimethylaminopyridine (4.27 g, 35 mmol) in 20 mL of pyridine was heated at 110 °C overnight. The reaction mixture was partitioned with EtOAc and H_2O. The organic phase was dried (Na_2SO_4) and concentrated in vacuo to give 8.73 g of crude yellow solid. The crude product was triturated with petroleum ether to give 7.5 g of product as a white solid (yield = 73%). ^{1}H NMR (DMSO-d_6, 400 MHz) δ 7.40 (t, 1H, J = 7.92 Hz), 7.62 (d, 2H, J = 8.44 Hz), 7.83(d, 1 H, J = 7.41 Hz), 8.04 (d, 2 H, J = 8.44 Hz), 8.39 (d, 1 H, J = 8.31 Hz), 13.88 (s, 1H); LC/MS 297.02/299.10 $[M + H]^+$.

Step 2: Preparation of 2-(4-Chloro-2-fluorobenzyl)-3-(4-chlorophenyl)-7-(trifluoromethyl)-2*H*-indazole. A solution of 3-(4-chlorophenyl)-7-(trifluoromethyl)-1*H*-indazole (0.15 g, 0.506 mmol) and 2-chloro-4-fluorobenzyl bromide (0.134 g, 0.6 mmol) in DMF was heated at 120 °C overnight. The reaction mixture was partitioned with EtOAc and H_2O. The organic phase was washed with brine and concentrated in vacuo. The crude residue was purified by preparative HPLC (silica gel, Biotage 12M, solvent hexane/CH_2Cl_2, 1:1, flow rate 10 mL/min) to give 0.102 g of product as a white solid (yield = 46%). ^{1}H NMR (DMSO-d_6, 400 MHz) δ 5.77 (s, 2 H), 7.01 (t, 1H, J = 8.18 Hz), 7.23 (m, 2H), 7.40 (dd, 1H), 7.66 (m, 4H), 7.755 (dd, 1H), 7.83 (d, 1H, J = 8.45); MS (ES) m/z 439.1 $[M + H]^+$. HRMS: calcd for $C_{21}H_{12}Cl_2F_4N_2 + H^+$, 439.0386; found (ESI, $[M + H]^+$ obsd), 439.0390. Anal. ($C_{21}H_{12}Cl_2F_4N_2$) C, H, N. HPLC purity: 100%.

2-(2-Chloro-4-fluorobenzyl)-3-(4-chlorophenyl)-7-(trifluoromethyl)-2*H*-indazole (18). Reaction was performed according to the procedure of compound **17** from 3-(4-chlorophenyl)-7-(trifluoromethyl)-1*H*-indazole (0.15 g, 0.506 mmol) and 2-chloro-4-fluorobenzyl bromide (0.124 g, 0.6 mmol) to give 0.140 g of product (yield = 63%). ^{1}H NMR (DMSO-d_6, 400 MHz) δ 5.79 (s, 2 H), 6.92 (m, 1H), 7.16 (dt, 1 H), 7.24 (dt,, 1H), 7.43 (dd, 1H), 7.64 (m, 4H), 7.765 (dd, 1H), 7.836 (d, 1H, J = 8.44); MS (ES) m/z 439.1$[M + H]^+$. HRMS: calcd for $C_{21}H_{12}Cl_2F_4N_2 + H^+$, 439.0386; found (ESI, $[M + H]^+$ obsd), 439.0389. Anal. ($C_{21}H_{12}Cl_2F_4N_2$) C, H, N. HPLC purity: 98.9%.

2-(2-Chlorobenzyl)-3-(4-chlorophenyl)-7-(trifluoromethyl)-2*H*-indazole (19). Reaction was performed according to the procedure of compound **17** from 3-(4-chlorophenyl)-7-(trifluoromethyl)-1*H*-indazole (0.15 g, 0.50 mmol) and 2-chlorobenzyl bromide (0.133 g, 0.65 mmol) to give 0.056 g of product (yield = 27%). ^{1}H NMR (DMSO-d_6, 400 MHz) δ 5.76 (s, 2 H), 6.77 (dd, 1H), 7.26 (m, 2H), 7.4 (dd, 1H), 7.64 (m, 4H), 7.7 (dd, 1H), 7.87 (d, 1H, J = 8.45); MS (ES) m/z 421.1 $[M + H]^+$. HRMS: calcd for $C_{21}H_{13}Cl_2F_3N_2 + H^+$, 421.0483; found (ESI, $[M + H]^+$ obsd), 421.0481. Anal. ($C_{21}H_{13}Cl_2F_3N_2$) C, H, N. HPLC purity: 100%.

3-(4-Chlorophenyl)-2-(2-fluorobenzyl)-7-(trifluoromethyl)-2*H*-indazole (20). Reaction was performed according to the procedure of compound **17** from 3-(4-chlorophenyl)-7-(trifluoromethyl)-1*H*-indazole (0.15 g, 0.50 mmol) and 2-fluorobenzyl bromide (0.123 g, 0.65 mmol) to give 0.043 g of product (yield = 19%). ^{1}H NMR (DMSO-d_6, 400 MHz) δ 5.79 (s, 2 H), 6.94 (dt, 1H), 7.12 (m, 2H), 7.24 (dt, 1H), 7.31 (m, 1H), 7.645 (m, 4H), 7.75 (d, 1H, J = 7.01

Hz), 7.83 (d, 1H, $J = 8.45$); MS (ES) m/z 405.1 $[M + H]^+$. HRMS: calcd for $C_{21}H_{13}ClF_4N_2 + H^+$, 405.0779; found (ESI, $[M + H]^+$ obsd), 405.0776. Anal. ($C_{21}H_{13}ClF_4N_2$) C, H, N. HPLC purity: 100%.

3-(4-Chlorophenyl)-7-(trifluoromethyl)-2-[2-(trifluoromethyl)-benzyl]-2*H*-indazole (21). Reaction was performed according to the procedure of compound **17** from 3-(4-chlorophenyl)-7-(trifluoromethyl)-1*H*-indazole (0.15 g, 0.50 mmol) and 2-(trifluoromethyl-)benzyl bromide (0.155 g, 0.65 mmol) to give 0.054 g of product (yield = 24%). ^{1}H NMR (DMSO-d_6, 400 MHz) δ 5.92 (s, 2 H), 6.62 (d, 1H, $J = 7.79$ Hz), 7.28 (t, 1 H, $J = 7.8$ Hz), 7.49 (t, 1H, $J = 7.66$ Hz), 7.61 (m, 4H), 7.75 (d, 1H, $J = 7.27$ Hz), 7.80 (d, 1H, $J = 7.01$ Hz), 7.89 (d, 1H, $J = 8.44$); MS (ES) m/z 455.1 $[M + H]^+$. HRMS: calcd for $C_{22}H_{13}ClF_6N_2 + H^+$, 455.0751; found (ESI, $[M + H]^+$ obsd), 455.0744. Anal. ($C_{22}H_{13}ClF_6N_2$) C, H, N. HPLC purity: 100%.

3-(4-Chlorophenyl)-7-(trifluoromethyl)-2-[4-(trifluoromethyl)-benzyl]-2*H*-indazole (22). Reaction was performed according to the procedure of compound **17** from 3-(4-chlorophenyl)-7-(trifluoromethyl)-1*H*-indazole (0.15 g, 0.50 mmol) and 4-(trifluoromethyl)benzyl bromide (0.155 g, 0.65 mmol) to give 0.043 g of product (yield = 19%). ^{1}H NMR (DMSO-d_6, 400 MHz) δ 5.86 (s, 2 H), 7.21 (d, 2H, $J = 8.05$ Hz), 7.28 (dt, 1 H), 7.63 (m, 5H), 7.78 (d, 1H, $J = 7.02$ Hz), 7.86 (d, 1H, $J = 8.31$); MS (ES) m/z 455.1. HRMS: calcd for $C_{22}H_{13}ClF_6N_2 + H^+$, 455.0744; found (ESI, $[M + H]^+$ obsd), 455.0744. Anal. ($C_{22}H_{13}ClF_6N_2$) C, H, N. HPLC purity: 100%.

2-Benzyl-3-phenyl-7-(trifluoromethyl)-2*H*-indazole (5). 5 was prepared identically to the 4-fluoro (e.g., **11**) analogues starting from (2-fluoro-3-(trifluoromethyl)phenyl)(phenyl)methanone. ^{1}H NMR (DMSO-d_6, 400 MHz) δ 5.75 (s, 2H), 7.0 (dd, 2H), 7.26 (m, 4H), 7.58 (m, 5H), 7.75 (d, 1H, $J = 7.05$ Hz), 7.84 (d, 1H, $J = 8.46$). HRMS: calcd for $C_{21}H_{15}F_3N_2 + H^+$, 353.1260; found (ESI, $[M + H]^+$ obsd), 353.1267. Anal. ($C_{21}H_{15}F_3N_2$) C. HPLC purity: 100%.

Seven Day Hamster Model. The 5−6 week old (90−100 g) male Golden Syrian hamsters were obtained from Harlan (Indianapolis IN). Hamsters were randomized by body weight and group and housed two per cage in plastic cages with ad libitum access to water and diet (Purina Rodent Chow 5001). Animals were allowed to acclimate for 1 week under standard conditions with a 12 h/12 h light/dark cycle (lights on at 0600 h) and with temperature controlled at 22 ± 2 °C. All experimental procedures were performed according to protocols approved by the Wyeth Institutional Animal Care and Use Committee (Collegeville, PA). Animals were divided into four groups ($n = 6$ per group) and were dosed once daily by oral gavage with vehicle (0.5% methylcellulose/2.0% Tween-80) or vehicle containing compound at a concentration designed to deliver a target dose of either 3 (mg/kg)/day for **3** or 100 (mg/kg)/day for **13**. On the final day, food was removed at time of final dosing. Two hours later the animals were euthanized. RNA was prepared from duodenum and liver and quantified by real time PCR. All gene expression values were normalized for glyceraldehyde-3-phosphate dehydrogenase (GAPDH) expression, with the expression seen in vehicle treated animals defined as 1.0 for each gene. Whole blood was collected into serum separator tubes, and serum was isolated and analyzed for total cholesterol, triglycerides, AST, and ALT using enzymatic methods. Plasma total cholesterol and triglyceride were determined using a Roche 912 clinical chemistry analyzer.

For hepatic triglyceride analysis, 200 mg of frozen liver was homogenized in 10 mL of 2:1 chloroform/methanol, stored under nitrogen, and shaken overnight. Then 4 mL of water was added and the samples were centrifuged at 500*g* for 20 min. The organic phase was filtered through cheesecloth and centrifuged at 500*g* for 10 min, and a portion (0.5 mL) was evaporated under nitrogen. The samples were resuspended in 2.5 mL of 30 mM pipes, pH 7.0, 60 mM $MgCl_2$, 0.1% NP-40 by sonication, stored under nitrogen, and shaken overnight. Then 0.2 mL of resuspended sample was treated with 10 μg of lipase (*Pseudomonas* sp., Sigma) at 37 °C for 1 h. An amount of 80 μL of sample was transferred to a clear 96-well plate and incubated with 160 μL of Free glycerol reagent (Sigma) for 10 min. The absorbance at 540 nm was determined, compared to a glycerol standard curve, and converted into a triolein mg/mL equivalent. In parallel with samples, 400 μg of triolein was added to control liver extracts and processed to determine recovery efficiency.

In Vitro Assays. LXRα and LXRβ binding assays (Table 1), Gal4 transactivation assays (Table 1), ABCA1 gene regulation in THP-1 cells (Table 2), C-efflux (Table 2), and SREBP1c in HepG2 cells (Table 2) were performed as described previously.[9] NHR cross-reactivity assays and data are outlined in Supporting Information.

TG Accumulation in HepG2 Cells. Results for compounds in Table 2 were obtained using methods previously described.[24]

LDL KO Mouse Inhibition of Lesion Progression Model. Eight-week old male LDLRKO were fed atherogenic diet or diet supplemented to deliver **2**, **3**, or **13** for 8 weeks. Aortas were obtained and analyzed using methods previously described.[9]

X-ray Crystal Structure of 12 with LXRβ LBD. Results were obtained using methods as previously described.[9]

Acknowledgment. We thank the Wyeth Discovery Analytical Chemistry Department for the analytical data, and Liang Chen, Anita Halpern, Qiang Liu, Johnny Sandberg, and Dawn Savio for biological assay data, and Dr. Baihua Hu for resynthesis of compound **13**. We also thank Dr. Magid Abou-Gharbia for his support of this work.

Supporting Information Available: Additional analytical data for compounds **5** and **11**−**21** and cross-reactivity data for compounds **12** and **13**. This material is available free of charge via the Internet at http://pubs.acs.org.

References

(1) Kalaany, N. Y.; Mangelsdorf, D. J. LXRs and FXR: The Yin and Yang of Cholesterol and Fat Metabolism. *Annu. Rev. Physiol.* **2006**, *68*, 159–191.

(2) Beaven, S. W.; Tontonoz, P. Nuclear Receptors in Lipid Metabolism: Targeting the Heart of Dyslipidemia. *Annu. Rev. Med.* **2006**, *57*, 313–329.

(3) Michael, L. F.; Schkeryantz, J. M.; Burris, T. The Pharmacology of LXR. *Mini-Rev. Med. Chem.* **2005**, *5*, 729–740.

(4) Bruemmer, D.; Law, R. E. Liver X Receptors: Potential Novel Targets in Cardiovascular Diseases. *Curr. Drug Targets: Cardiovasc. Haematol. Disord.* **2005**, *5*, 533–540.

(5) Tangirala, R. K.; Bischoff, E. D.; Joseph, S. B.; Wagner, B. L.; Walczak, R.; Laffitte, B. A.; Daige, C. D.; Thomas, D.; Heyman, R. A.; Mangelsdorf, D. J.; Wang, X.; Lusis, A. J.; Tontonoz, P.; Schulman, I. G. Identification of Macrophage Liver X Receptors as Inhibitors of Atherosclerosis. *Proc. Natl. Acad. Sci. U.S.A.* **2002**, *99* (18), 11896–11901.

(6) Joseph, S. B.; McKilligin, E.; Pei, L.; Watson, M. A.; Collins, A.; Laffitte, B. A.; Chen, M.; Noh, G.; Goodman, J.; Hagger, G. N.; Tran, J.; Tippin, T. K.; Wang, X.; Lusis, A. J.; Hsueh, W. A.; Law, R. E.; Collins, J. L.; Willson, T. M.; Tontonoz, P. Synthetic LXR Ligand Inhibits the Development of Atherosclerosis in Mice. *Proc. Natl. Acad. Sci. U.S.A.* **2002**, *99*, 7604–7609.

(7) Schultz, J. R.; Tu, H.; Luk, A.; Repa, J. J.; Medina, J. C.; Li, L. P.; Schwendner, S.; Wang, S.; Thoolen, M.; Mangelsdorf, D. J.; Lustig, K. D.; Shan, B. Role of LXRs in Control of Lipogenesis. *Genes Dev.* **2000**, *14* (22), 2831–2838.

(8) Collins, J. L.; Fivush, A. M.; Watson, M. A.; Galardi, C. M.; Lewis, M. C.; Moore, L. B.; Parks, D. J.; Wilson, J. G.; Tippin, T. K.; Binz, J. G.; Plunket, K. D.; Morgan, D. G.; Beaudet, E. J.; Whitney, K. D.; Kliewer, S. A.; Willson, T. M. Identification of a Nonsteroidal Liver X Receptor Agonist through Parallel Array Synthesis of Tertiary Amines. *J. Med. Chem.* **2002**, *45*, 1963–1966.

(9) Hu, B.; Collini, M.; Unwalla, R.; Miller, C.; Singhaus, R.; Quinet, E.; Savio, D.; Halpern, A.; Basso, M.; Keith, J.; Clerin, V.; Chen, L.; Resmini, C.; Liu, Q.-Y.; Feingold, I.; Huselton, C.; Azam, F.; Farnegardh, M.; Enroth, C.; Bonn, T.; Goos-Nilsson, A.; Wilhelmsson, A.; Nambi, P.; Wrobel, J. Discovery of Phenyl Acetic Acid Substituted Quinolines as Novel Liver X Receptor Agonists for the Treatment of Atherosclerosis. *J. Med. Chem.* **2006**, *49*, 6151–6154.

(10) Hu, B.; Jetter, J.; Kaufman, D.; Singhaus, R.; Bernotas, R.; Unwalla, R.; Quinet, E.; Savio, D.; Halpern, A.; Basso, M.; Keith, J.; Clerin, V.; Chen, L.; Liu, Q.-Y.; Feingold, I.; Huselton, C.; Azam, F.; Goos-

Nilsson, A.; Wilhelmsson, A.; Nambi, P.; Wrobel, J. Further Modifications on Phenyl Acetic Acid Based Quinolines as Liver X Receptor Modulators. *Bioorg. Med. Chem.* **2007**, *15*, 3321–3333.

(11) Nambi, P.; Basso, M.; Chen, L.; Liu, Q.; Keith, J.; Clerin, V.; Quinet, E.; Savio, D.; Halpern, A.; Wrobel, J. WAY-254011 Inhibits Atherosclerotic Lesion Progression and Inflammatory Markers in the LDL Receptor Knockout Mice. Presented at the Keystone Meeting, Nuclear Receptors: Orphan Brothers (X3), Banff, Alberta, Canada, 2006.

(12) Nambi, P.; Basso, M.; Chen, L.; Liu, Q.; Clerin, V.; Feldman, J.; Pitman, D.; Keith, J.; Quinet, E.; Wrobel, J. WAY-254011, a Novel LXR Modulator, Inhibits Atherosclerotic Lesion Progression in ApoE Knockout Mice. Presented at the XIV International Symposium on Atherosclerosis, Rome, Italy, 2006.

(13) Quinet, E.; Savio, D.; Halpern, A.; Chen, L.; Schuster, G. U.; Gustafsson, J.; Basso, M.; Nambi, P. Liver X Receptor (LXR)—Regulation in LXR-Deficient Mice: Implications for Therapeutic Targeting. *Mol. Pharmacol.* **2006**, *70*, 1340–1349.

(14) Lund, E. G.; Peterson, L. B.; Adams, A. D.; Lam, M. N.; Burton, C. A.; Chin, J.; Guo, Q.; Huang, S.; Latham, M.; Lopez, J. C.; Maenke, J. G.; Milot, D. P.; Mitnaul, L. J.; Rex-Rabe, S. E.; Rosa, R. L.; Tian, J. Y.; Wright, S. D.; Sparrow, C. P. Different Roles of Liver X Receptor α and β in Lipid Metabolism: Effects of an α-Selective and a Dual Agonist in Mice Deficient in Each Subtype. *Biochem. Pharmacol.* **2006**, *71*, 453–463.

(15) Scott, J. The Liver X Receptor and Atherosclerosis. *N. Engl. J. Med.* **2007**, *357* (21), 2195–2197.

(16) Bradley, M. N.; Hong, C.; Chen, M.; Joseph, S. B.; Wilpitz, D. C.; Wang, X.; Aldons, J. L.; Collins, A.; Hseuh, W. A.; Collins, J. L.; Tangirala, R. K.; Tontonoz, P. Ligand Activation of LXRβ Reverses Atherosclerosis and Cellular Cholesterol Overload in Mice Lacking LXRα and apoE. *J. Clin. Invest.* **2007**, *117*, 2337–2346.

(17) Wrobel, J.; Steffan, R. J.; Matelan, E.; Bowen, S. M.; Hu, B.; Collini, M.; Miller, C. P.; Unwalla, R. J.; Nambi, P.; Quinet, E.; Chen, L.; Halpern, A.; Liu, Q.-Y.; Savio, D.; Zamaratsky, E.; Kruger, L.; Wilhelmsson, A.; Goos Nilsson, A.; Ursu, C.; Arnelof, E.; Sandberg, J.; Enroth, C.; Farnegardh, M. Discovery of LXR Modulator WAY-252623. Presented at the 234th National Meeting of the American Chemical Society, Boston, MA, 2007.

(18) Nambi, P.; Basso, M. D.; Chen, L.; Liu, Q.-Y.; Halpern, A.; Clerin, V.; Resmini, C.; Keith, J.; Feingold, I.; Steffan, R. J.; Wrobel, J.; Quinet, E. Abstract 1453: LXR-623, a Novel Liver X Receptor Modulator, Displays Neutral Lipid Effects in Cholesteryl Ester Transfer Protein-Expressing Species and Inhibits Atherosclerotic Lesion Progression in Low Density Lipoprotein Receptor Knockout Mice. *Circulation* **2007**, *116*, 299.

(19) Figures were made using the program INSIGHT II, version 2005 (Accelrys, San Diego, CA).

(20) Faernegardh, M.; Bonn, T.; Sun, S.; Ljunggren, J.; Ahola, H.; Wilhelmsson, A.; Gustafsson, J.-A.; Carlquist, M. The Three-Dimensional Structure of the Liver X Receptor β Reveals a Flexible Ligand-Binding Pocket That Can Accommodate Fundamentally Different Ligands. *J. Biol. Chem.* **2003**, *278*, 38821–38828.

(21) Wouters, K.; Shiri-Sverdlov, R.; van Gorp, P. J.; van Bilsen, M.; Hofker, M. H. Understanding Hyperlipidemia and Atherosclerosis: Lessons from Genetically Modified ApoE and LDLr Mice. *Clin. Chem. Lab. Med.* **2005**, *43*, 470–479.

(22) Groot, P. H.; Pearce, N. J.; Yates, J. W.; Stocker, C.; Sauermelch, C.; Doe, C. P.; Willette, R. N.; Olzinski, A.; Peters, T.; d'Epagnier, D.; Morasco, K. O.; Krawiec, J. A.; Webb, C. L.; Aravindhan, K.; Jucker, B.; Burgert, M.; Ma, C.; Marino, J. P.; Collins, J. L.; Macphee, C. H.; Thompson, S. K.; Jaye, M. Synthetic LXR Agonists Increase LDL in CETP Species. *J. Lipid Res.* **2005**, *46*, 2182–2191.

(23) Plasma TG levels for compound **3** at 10 (mg/kg)/day were 395 ± 53 mg/dL and at 30 (mg/kg)/day were 913 ± 68 mg/dL.

(24) Hu, B.; Quinet, E.; Unwalla, R.; Collini, M.; Jetter, J.; Dooley, R.; Andrake, D.; Nogle, L.; Savio, D.; Halpern, A.; Goos-Nilsson, A.; Wilhelmsson, A.; Nambi, P.; Wrobel, J. Carboxylic Acid Based Quinolines as Liver X Receptor Modulators That Have LXRβ Receptor Binding Selectivity. *Bioorg. Med. Chem. Lett.* **2008**, *18* (1), 54–59.

JM800799Q